Version 2008-04-09 Resubmission to Journal of Applied Remote Sensing

Intercomparison of Near-Real-Time Biomass Burning Emissions Estimates Constrained by Satellite Fire Data

Jassim Al-Saadi,[a] Amber Soja,[b] R. Bradley Pierce,[c] James Szykman,[d] Christine Wiedinmyer,[e] Louisa Emmons,[e] Shobha Kondragunta,[f] Xiaoyang Zhang,[f] Chieko Kittaka,[g] Todd Schaack,[h] Kevin Bowman[i]

[a]NASA Langley Research Center, Hampton, VA
j.a.al-saadi@nasa.gov
[b]National Institute of Aerospace, Hampton, VA
[c]NOAA NESDIS, Madison, WI
[d]US EPA, Research Triangle Park, NC
[e]NCAR, Boulder, CO
[f]NOAA NESDIS, Camp Springs, MD
[g]SSAI, Hampton, VA
[h]Space Science and Engineering Center, University of Wisconsin, Madison WI
[i]Jet Propulsion Laboratory, Pasadena, CA

Abstract. We compare biomass burning emissions estimates from four different techniques that use satellite based fire products to determine area burned over regional to global domains. Three of the techniques use active fire detections from polar-orbiting MODIS sensors and one uses detections and instantaneous fire size estimates from geostationary GOES sensors. Each technique uses a different approach for estimating trace gas and particulate emissions from active fires. Here we evaluate monthly area burned and CO emission estimates for most of 2006 over the contiguous United States domain common to all four techniques. Two techniques provide global estimates and these are also compared. Overall we find consistency in temporal evolution and spatial patterns but differences in these monthly estimates can be as large as a factor of 10. One set of emission estimates is evaluated by comparing model CO predictions with satellite observations over regions where biomass burning is significant. These emissions are consistent with observations over the US but have a high bias in three out of four regions of large tropical burning. The large-scale evaluations of the magnitudes and characteristics of the differences presented here are a necessary first step toward an ultimate goal of reducing the large uncertainties in biomass burning emission estimates, thereby enhancing environmental monitoring and prediction capabilities.

Keywords: biomass burning, emission, wildfire, atmospheric composition

1 INTRODUCTION

Biomass burning is a major contributor of particulate matter and trace gases to the global troposphere. Burning is also subject to large interannual variability [1]. Together, these two facts define both the fundamental importance of and difficulty in establishing accurate biomass burning emissions inventories. The problem is further compounded by differing temporal and spatial requirements. Air quality modeling at the regional and local level requires that emissions be resolved at diurnal or even hourly scales. Further, large fires are capable of lofting emissions into the upper troposphere, where strong winds can result in inter-regional and intercontinental transport of these emissions within a few days [2][3]. In these situations there is potential for local air quality to be significantly influenced by events outside the domain of regional air quality models [4][5].

An approach for addressing this variability in biomass burning emissions is to calculate spatially and temporally accurate emissions based on observations of active fires. Satellite observations provide a consistent means of detecting active burning at continental to global scales. Geostationary platforms, such as the NOAA GOES satellites, can provide continuous observations over regional domains, making it possible to detect short duration fires and also to resolve the diurnal behavior of large fires. Polar orbiting satellites, including the NASA Terra and Aqua satellites, offer global coverage but typically provide only one daytime and one nighttime observation every 24 hours.

Here we begin to assess the uncertainties in current biomass burning emission estimates constrained by satellite-based fire products. We first introduce a new technique for generating daily global biomass burning emissions estimates in near real time for use in atmospheric composition forecasts. We then intercompare 2006 estimates of area burned and biomass burning CO emissions generated from four different methods using detections of active fires from either polar-orbiting or geostationary satellites. We evaluate CO emissions by comparing model CO predictions with satellite observations in regions where biomass burning is significant. Most of the analysis focuses on the contiguous US (CONUS) where the product based on half-hourly geostationary GOES observations is available. We also briefly evaluate global results from the two global techniques to additionally consider factors controlling biomass burning emissions in ecosystems and conditions not found over CONUS.

2 BIOMASS BURNING EMISSIONS TECHNIQUES

In this paper we compare four different techniques that use satellite-based fire products to produce emissions estimates. The techniques are summarized in Table 1. Two of the techniques are global and two are regional. Both global techniques use MODIS active fire detections, although at different levels of processing. One regional technique uses MODIS detections and one uses processed GOES detections. The new technique used in the NASA/University of Wisconsin Realtime Air Quality Modeling System (RAQMS) [6][7][8] is described here in some detail, while the three other emissions techniques have each been described in the literature so only very brief summaries are given here.

2.1 RAQMS Emissions

The technique described here was developed to provide daily emissions for RAQMS forecasts that were used to support flight planning and data analysis during the March-May 2006 NASA INTEX-B and August-October 2006 NOAA TexAQS field campaigns. These forecasts were also used as lateral boundary conditions for regional air quality predictions with the University of Iowa STEM model [9], demonstrating a capability for global-to-regional assessment of burning influences on air quality.

The basic approach [10] relies on gridded carbon fuel consumption databases, satellite fire detections, and meteorology-based estimates of fire weather severity to estimate the amount of carbon released from active fires. Emissions of CO, NOx, and hydrocarbons are then estimated using ecosystem-dependent emission ratios. The ecosystem-dependent carbon consumption databases represent the amounts of carbon released from burning of vegetation and sequestered fuel [11][12][13] and have been generated for three classes of fire severity (low, medium, high). We estimate fire weather severity using the US Forest Service Haines Index [14]. The Haines Index considers atmospheric moisture and thermal stability in the lower free troposphere to characterize the potential for atmospheric instability to bring dry air to the ground, a process particularly associated with sudden increases in fire activity such as towering plume-dominated fires [15]. The Index gives an indication of the potential for the rate of spread of a fire on a given day. We calculate the Index daily over the entire globe using the 6-hourly meteorological analysis (i.e., 00Z, 06Z, 12Z, 18Z) that is closest in time to

Table 1. Basic characteristics of the 2006 biomass burning emission products used in this study.

	NASA Global (RAQMS)	NCAR Global (MOZART)	NCAR Regional	NOAA GOES
Domain	Global	Global	North+Central America	CONUS
Satellite Fire Detection	MODIS Rapid Response	MODIS Climate Modeling Grid	MODIS Rapid Response	GOES processed half-hourly
Area Burned Estimate	$1km^2$ for each unique Terra+Aqua detect in running 48-hr window	GFEDv2 scaled by Terra 8-day Climate Modeling Grid detects	Vegetated fraction of $1km^2$ from combined Terra+Aqua detects	Simulated from WF_ABBA subpixel algorithm
Emissions Estimate	Calculated from fire severity-based carbon consumption databases (Haines Index for severity estimate) and published emission ratios	GFEDv2 scaled by Terra 8-day Climate Modeling Grid detects	Calculated from biomass fuel loading databases, MODIS vegetation products, and published emission ratios	Calculated from fuel loading databases, combustion efficiency parameters, and emission factors from FOFEM model
2006 Dates of Coverage	Feb 1 – Oct 15	Jan 1 – Dec 31	Jan 1 – Dec 31	Mar 1 – Sep30
Horizontal Resolution	1 deg x 1 deg	1 deg x 1 deg	1 km (MODIS nadir pixel size)	4 km (GOES nadir pixel size)
Temporal Resolution	Daily	8-days	Daily	Daily
Species available in this intercomparison	CO, NO, area-burned	CO, NO, CO2, CH4, PM2.5, area-burned	CO, CO2, CH4, PM2.5, VOC, NOx, area-burned	CO, area-burned
Other species typically produced	C; other species (NMHC, aerosol) calculated from C	Other species calculated from CO2	PM10, HCN, CH3CN, NH3, SO2, Hg	PM2.5, CH4

local noon. We use the high severity carbon consumption database where the Haines Index is 6, medium severity where the Index is 5, and low severity where the Index is 4 or less.

Our need to generate global emissions in all ecosystems in near real time dictates the use of MODIS Rapid Response fire detections [16] for estimating fire location, timing, and area burned. Yet there is large uncertainty in inferring area burned from active fire detections, and additional sources of uncertainty include missing fire detections (e.g., due to cloud cover or to short duration fires occurring when there is no satellite overpass), false detections, and multiple detections of the same fire [17][18]. We use instantaneous active fire detections from the two MODIS instruments onboard the NASA Terra and Aqua satellites. Each instrument provides one daytime and one nighttime observation of most of the globe at a nominal 1 km x 1 km horizontal resolution. At present we create separate day and night emissions estimates, using corresponding day and night MODIS detections, to account for diurnal fire behavior. Daily and nightly total direct carbon emissions are then calculated as the product of area burned and the ecosystem- and severity-specific carbon consumption estimates within each 1x1 degree grid cell. Emissions of other species are determined by combining published emission ratios for different ecosystems [19][20].

Due to the orbital characteristics of Terra and Aqua and the swath width (footprint) of the MODIS instruments, locations at equatorial regions may be viewed only once every other day. Conversely, convergence of orbit tracks at high latitudes provides multiple viewing opportunities of mid and high latitudes per day, raising the possibility of multiple detections

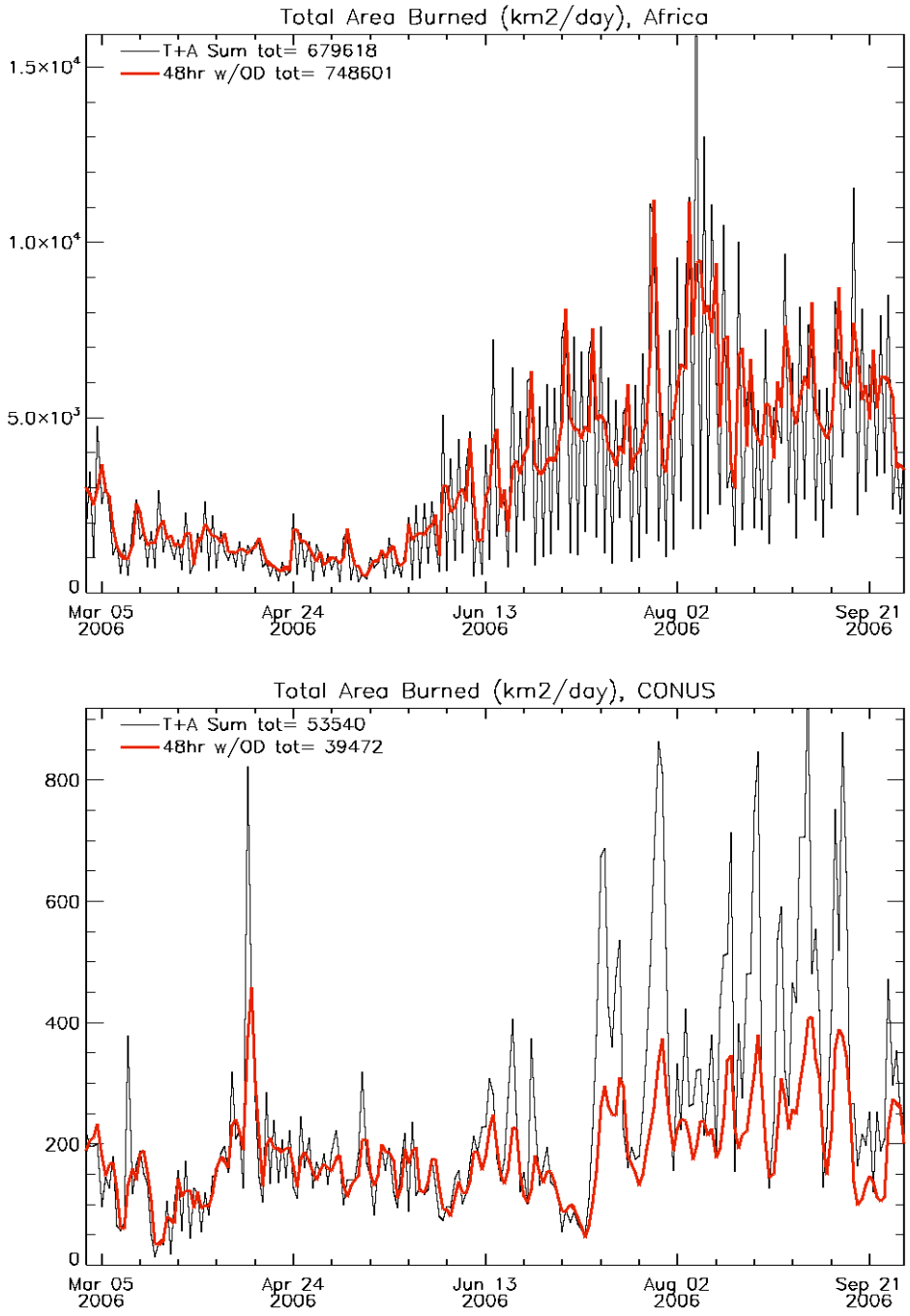

Fig. 1. Time series of daily area burned estimates integrated over Africa and the contiguous US (CONUS) from March 1 through September 30, 2006. Shown are area estimates resulting from summing all Terra and Aqua fire counts during a 24 hour period (black line) and from the current technique (red line).

of the same fire. Combining Terra and Aqua also presents the possibility of multiple detections at all latitudes. We are presently conducting research into ways of processing the active MODIS fire detections to minimize these sampling biases in daily estimates. In the technique presented here, 48 hours of MODIS Terra and Aqua data are aggregated to ensure complete coverage over equatorial regions, while multiple detections of the same fire (i.e., within the same nominal 1 km x 1 km pixel area) are identified and removed. This processing yields a daily global distribution of MODIS pixels in which a fire has been detected.

The relationship between MODIS fire detections and area burned is complex and varies with parameters including vegetation type and fire size [21]. We make the ad-hoc assumption that each unique MODIS fire detection corresponds to an area burned of 1 km^2 over 24 hours. In grassland ecosystems (which includes cropland in our parameterization) we use a smaller value (0.75 km^2 per 24 hours) corresponding to an assumed shorter duration for fires in such ecosystems. Giglio et al. [21] use burn scar data and fire detections from MODIS Terra to show that in a simple linear regression the proportionality between detections and area burned ranges from 0.29 to 6.6 km^2 per detection globally. They calculate a mean value of 0.84 for CONUS (Temperate North America), including all ecosystems, which is consistent with our current assumptions of 0.75-1.0 depending on ecosystem. At present it is not known whether these relationships have any dependence on which MODIS platform is used for fire detections (Terra, Aqua, or both combined).

Fig. 1 demonstrates the behavior of this approach using time series of daily area burned estimates integrated over Africa and CONUS from March 1 through September 30, 2006. Shown are burn area estimates resulting from summing all Terra and Aqua fire counts during each 24 hour period (black line) and from the current technique (red line). Over Africa the daily sum shows a strong 2-day signature in which the minima result from gaps in satellite coverage while the maxima are apparently enhanced by multiple detections (i.e., Terra and Aqua see some of the same fires). The current technique has filtered much of this 2-day variability associated with biased sampling and has increased the total area burned estimate by about 10%. Over CONUS the largest impact of the current technique is a general reduction in area burned estimates during the peak summer burning season. This is to be expected since much of the burning in late summer is in the northwestern US, which is at high enough latitudes that there is overlap in the MODIS footprint between successive orbits and multiple detections of the same fires are possible.

2.2 NCAR Global Emissions

The NCAR Global technique was developed for retrospective (i.e., not forecast) global analyses with the MOZART model. This technique uses the Global Fire Emissions Database version 2 (GFEDv2) emissions and area burned estimates [1] scaled by MODIS Terra Climate Modeling Grid (CMG) fire detections [18]. The MODIS CMG 8-day fire products are gridded statistical summaries of fire detections over 8-day periods and are intended to remove the single-day sampling artifacts described above. A climatology of emissions per fire count was compiled by scaling the GFEDv2 emissions by MODIS fire counts for 2000-2004. The emission estimates shown here result from scaling this climatology using the 2006 Terra CMG detections at a horizontal resolution of 1x1 degrees.

2.3 NCAR Regional Emissions

The NCAR Regional technique was developed to provide high spatial resolution emissions at a daily temporal resolution over a domain including all of North and Central America [21]. The emissions were used in forecasts conducted with the MOZART and STEM models in support of the 2006 MILAGRO/INTEX-B field campaigns and the technique is currently used to provide emissions for the WRF-chem model. Emission estimates are generated for each active fire detection from MODIS Terra and Aqua. Area burned is assumed to be the fraction

of each nominal 1 km^2 pixel that is vegetated. Ecosystem-dependent biomass fuel loading databases, MODIS vegetation products, and published emission factors are used in deriving the emissions of several trace gases and particulates (Table 1).

2.4 NOAA GOES Emissions

The NOAA GOES emissions rely on fire detections associated with the Wild Fire Automated Biomass Burning Algorithm (WF_ABBA) [23][24]. Fire detections are processed every half hour at the nominal horizontal resolution of 4 km x 4 km. Every detection is assigned a fire flag value from 0 to 5 to indicate details such as confidence, cloud contamination, and sub-pixel processing. For about one third of the fire detections (flag value 0) the processing algorithm can calculate sub-pixel fire characteristics including estimation of instantaneous fire size [25]. Recent work has focused on deriving fire size estimates for the remainder of high-confidence detections and improving the estimation of area burned from the instantaneous fire size estimates [26]. Emission estimates are calculated from these area burned estimates, fuel loading databases [27], combustion efficiency parameters, and emission factors from the First Order Fire Effects Model (FOFEM) [28].

3 RESULTS

We analyze two of the basic products common to each of the techniques: area burned and CO emissions. For all results shown here the area burned and emission estimates from the two regional models have been aggregated from their native resolutions (1 km x 1 km NCAR Regional, 4 km x 4 km NOAA GOES) to a 1x1 degree grid.

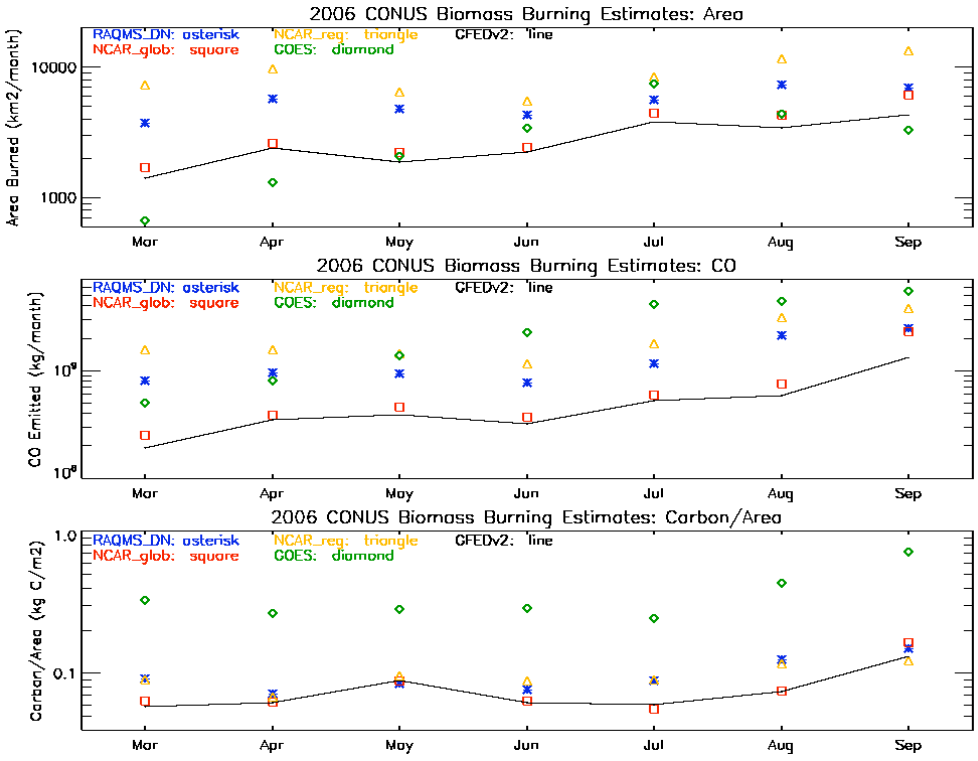

Fig. 2 Monthly biomass burning estimates integrated over the contiguous United States during 2006. Top panel: area burned. Middle panel: CO emission. Bottom panel: ratio of carbon emission per unit area burned.

3.1 Comparison of techniques over CONUS

Fig. 2 shows monthly estimates from each of the techniques integrated over CONUS during 2006. Also shown for reference are 2006 monthly values from GFEDv2, a MODIS-derived product that is not available in near real time [1]. Within any particular month there is up to an order of magnitude spread in the area burned (top panel) and CO emission (middle panel) estimates. The three methods using MODIS fire detections have consistent relationships with each other for both area burned and CO emission in that values from NCAR Regional are largest of the three and from NCAR Global are smallest of the three. These relationships appear consistent with the different treatments of MODIS detections and subsequent estimates of area burned. NCAR Regional accumulates all Terra and Aqua detects with no overlap detection and has the largest values. The GFEDv2 database used by NCAR Global uses a regression-tree approach to derive area from MODIS fire detections [21] and, as noted above, a mean factor of 0.84 km^2/pixel was found for temperate North America versus the nominal factor of 1.0 used in NCAR Regional and RAQMS. RAQMS, with Terra/Aqua overlap detection, yields intermediate values. The NCAR Global estimates are very similar to the GFEDv2 values, differing notably only in September, and this reproducibility shows that scaling climatological values by fire detections is a reasonable approach for estimating near real time emissions. The GOES technique shows the strongest seasonal cycle in both area burned and CO emission. The area burned estimates are similar to the MODIS-based estimates from May through August and are lower during March, April, and September. GOES-based CO emissions are largest of all techniques from June through September.

The bottom panel of Fig. 2 shows the ratio of carbon emitted to area burned. In these mean statistics the GOES technique has consistently larger values of carbon emission per unit area. The MODIS-based approaches show values of carbon emission per unit area that are similar to each other in spite of the different methods for determining CO emissions. Next we focus on two months to analyze details of these comparisons. We look at March, the period of largest disagreement in both area and CO, and July, a period of good agreement in estimated area burned with large CO emissions and a large range of CO emissions.

Fig. 3(a) shows 1-degree maps of area burned from each technique during March 2006. White regions show where no fires were detected. The spatial patterns are reasonably consistent as all methods show that most burning is occurring in the southeastern and south central US and show peak burning in north Texas and the Florida panhandle. GOES has fewer detections in the northern US, particularly the Pacific Northwest. Although the spatial patterns are similar in the southeast, it is clear that the GOES estimates are smaller than the MODIS-based estimates. Much of the burning in the southeast during this time is associated with small-scale agricultural fires and prescribed burning [29]. The duration of such fires is on the order of hours rather than days. The short duration and small size accentuate differences between MODIS and GOES with respect to the likelihood of fire detection and estimation of burned area. Because of the differences in sensor spatial resolution, it would generally be expected that MODIS (1 km^2 nadir resolution) is capable of detecting smaller fires than GOES (16 km^2 nadir resolution). However, the continuous observations from GOES allow detection of shorter duration fires that may not be burning at the less frequent overpass times of MODIS. Further, the GOES area burned estimates (based on the half-hourly sub-pixel fire size algorithm) are often much smaller than the 1 km^2 pixel resolution of MODIS, whereas the MODIS-based techniques assume burn areas of approximately 1 km^2 per detection.

Fig. 3(b) shows maps of the CO emissions for March. The CO emissions appear more consistent among the techniques than the area estimates. Largest emissions and largest differences are in the southeast. Shown in Fig. 3(c) are maps of carbon emissions per unit area. Order-of-magnitude differences are apparent in most of the southeast, where GOES values are typically the highest, values from RAQMS and NCAR Regional are quite similar to each other, and values from NCAR Global show much more heterogeneity than the other

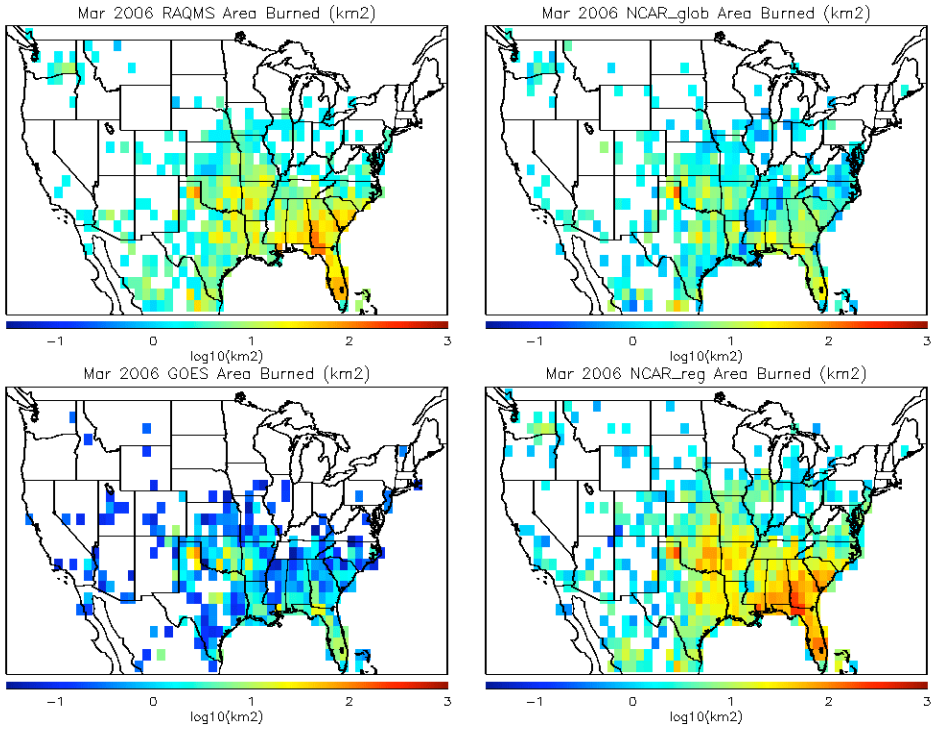

Fig. 3 Maps of biomass burning estimates from each technique during March 2006.
(a) Area burned estimates.

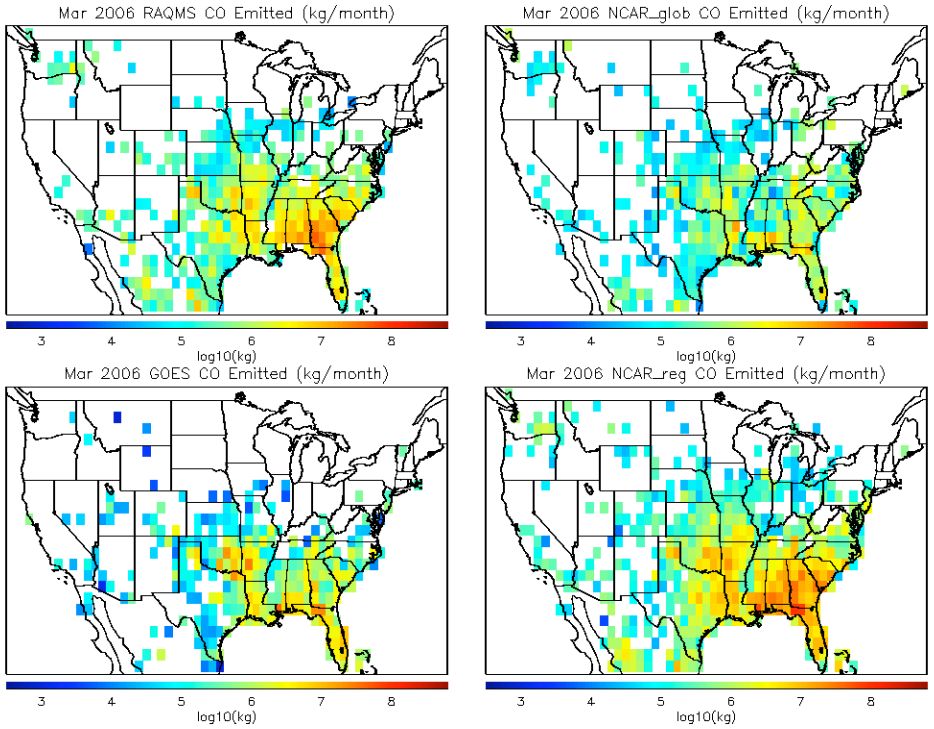

Fig. 3 Continued. (b) Carbon monoxide emission estimates.

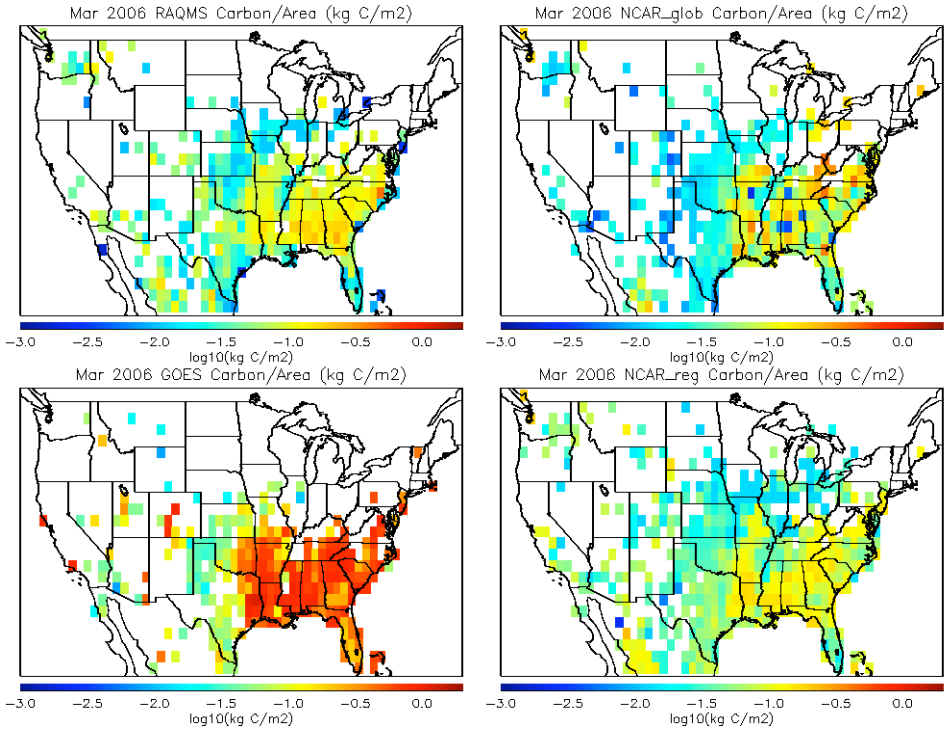

Fig. 3 Concluded. (c) Ratio of carbon emitted to area burned.

methods. NCAR Global values in the southeast range from the lowest of all models to among the highest of the MODIS-based methods. In the central US the emission per unit area is smaller and is more consistent among the models. Variation in this quantity is highlighting differences in the details of the emission models, including ecosystem and vegetation dependences of emission factors and fuel loadings.

Fig. 4(a) shows maps of area burned in July. The GOES method produces some 1-degree cells containing fire detections in the Midwest, Plains, and Rocky Mountain regions that are not captured by MODIS. These detections are associated with very small area burned estimates. Again, this difference is probably due to the more frequent observations from GOES, which allow detection of short duration fires that are either not burning or not visible (due to clouds) at the times of MODIS overpasses. All methods appear to produce similar estimates in regions with large area burned (West Coast, Northern Plains). This similarity in the estimates in regions of large area burned leads to the good agreement in overall burned area seen in Fig. 2 during July since large areas dominate the totals. The CO emissions for July are shown in Fig. 4(b). There is good spatial consistency among the techniques as regions of high emissions are similarly captured by all methods. In regions of largest emissions (northwest and southeast) the NCAR Global emissions are smaller than the other methods while in the 1-degree cells with highest emissions the GOES values are typically the largest. July emission per unit area is shown in Fig. 4(c). All methods show large values of this ratio in the southeast and northwest. Beyond this spatial similarity there is less consistency among the techniques in the actual values of this ratio than was seen in March, although as seen in March the values from the GOES method are larger than those from the MODIS methods in regions having the largest ratios. Land cover maps (not shown here) suggest that the locations where these ratios are the largest are associated with needle-leaf and broad-leaf forested ecosystems.

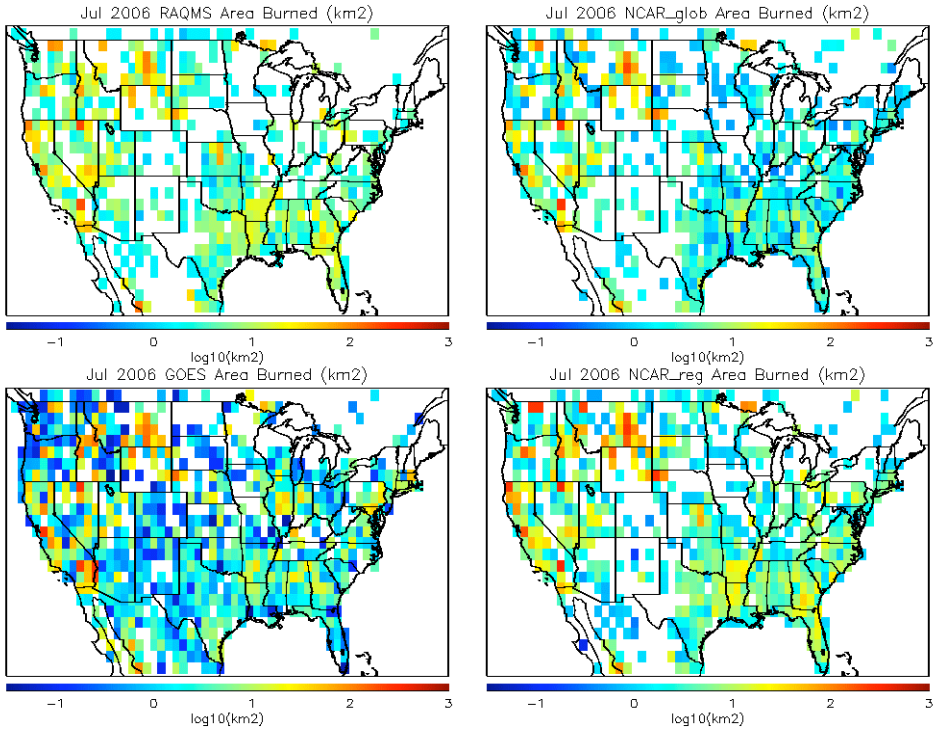

Fig. 4 Maps of biomass burning estimates from each technique during July 2006.
(a) Area burned estimates.

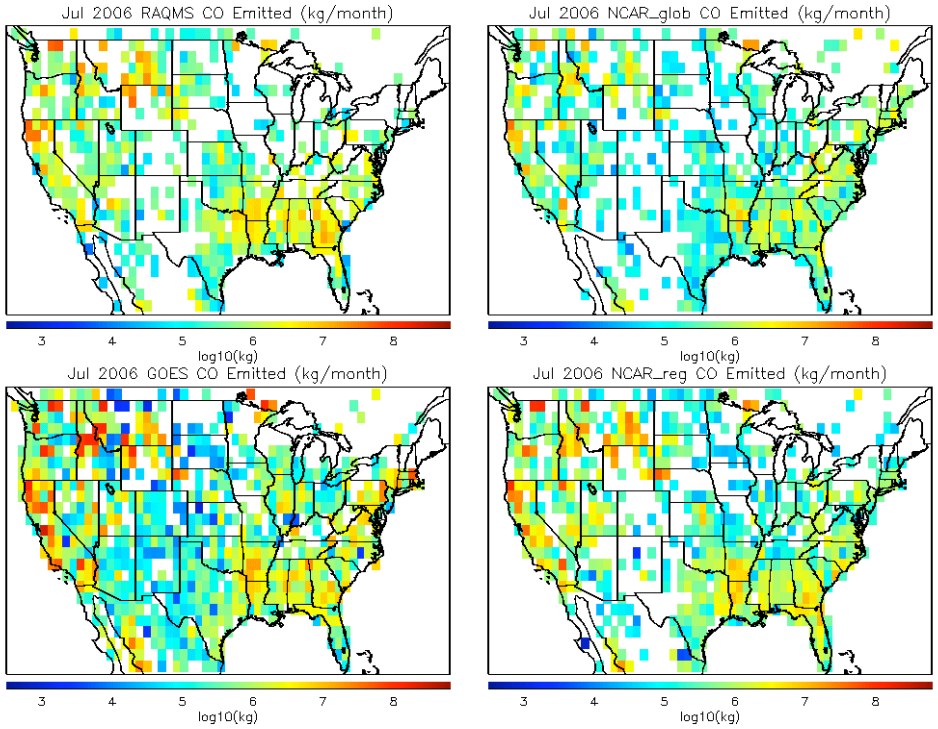

Fig. 4 Continued. (b) Carbon monoxide emission estimates.

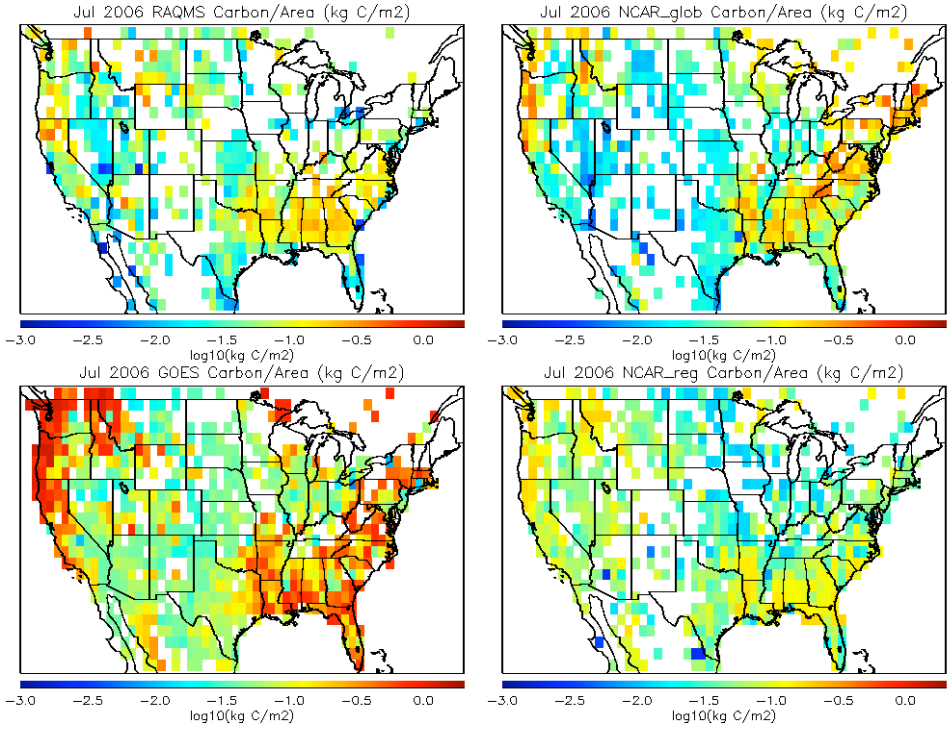

Fig. 4 Concluded. (c) Ratio of carbon emitted to area burned.

Summary histograms showing the frequency of occurrence of these 1-degree gridded quantities are considered next. March histograms of area burned, CO emission, and carbon emission ratio are shown in Fig. 5(a). Note that all distributions are shown on a logarithmic scale to capture the wide range of values present. Median values are shown as thin dashed lines. The area-burned distribution from the GOES product has a different shape than the MODIS products, shifted toward smaller values with a median value of 0.15 km^2. Median values for the other techniques range from 2.5 km^2 for NCAR Global to about 5 km^2 for NCAR Regional and RAQMS. The smallest value that can occur in the RAQMS product is 0.75 km^2. Both the NCAR Global and NCAR Regional methods have a population of values as small as about 0.3 km^2. More consistency is found in the histograms of CO emission. Both RAQMS and NCAR Regional have secondary peaks at high emission values while GOES has a relatively broad flat peak. Note that the rightmost portions of the histograms are consistent with the total March values shown in Fig. 2, showing that the largest fires and highest emissions dominate the monthly totals. The histograms of carbon emission per unit area show that GOES has a distinct population of points with high emission per unit area, consistent with the large values found in the southeastern US in Fig. 3(c). The GOES and NCAR Global techniques have bimodal distributions with the high-emission-ratio peak dominant in GOES and the low-emission-ratio peak dominant in NCAR Global, while NCAR Regional and RAQMS distributions are dominated by values between these two bimodal peaks. A final note is that these histograms show that overall there are fewer 1-degree cells with fire detections from the GOES product in March.

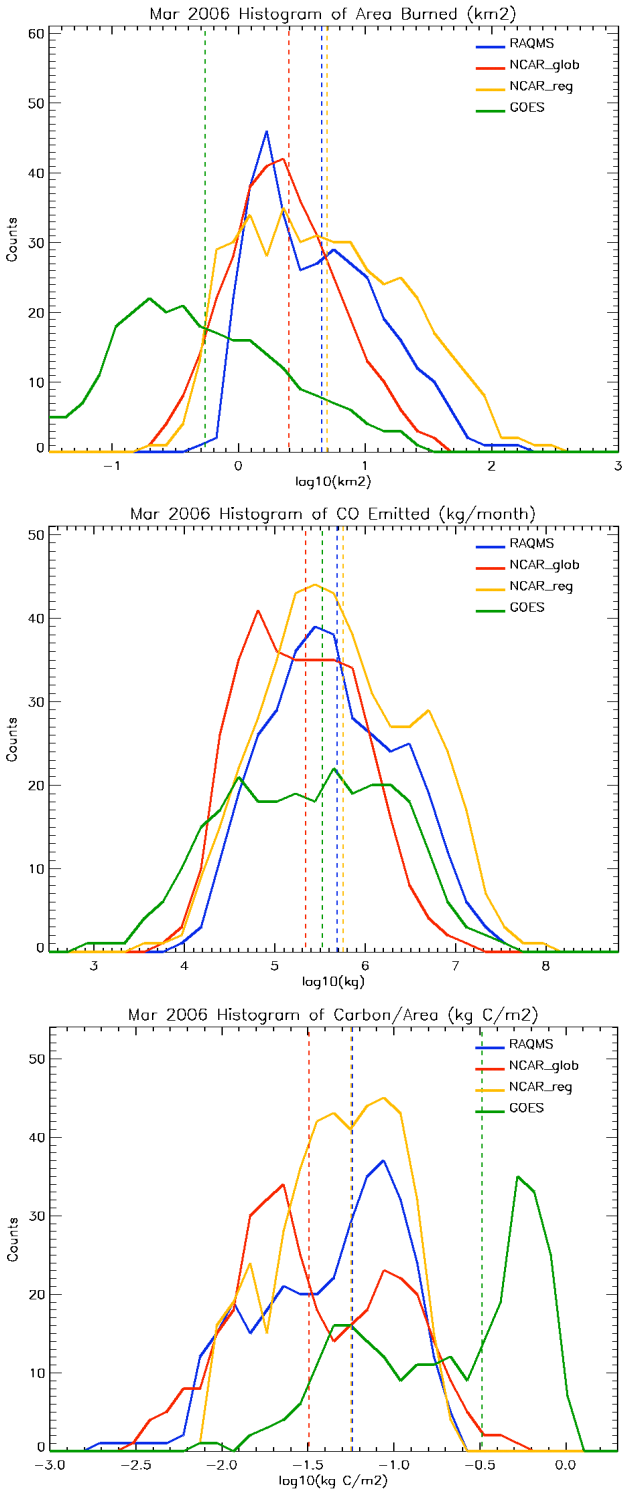

Fig. 5 Histograms of area burned, CO emitted, and net Carbon emission per unit area burned. Dashed lines indicate median values. Blue: RAQMS. Red: NCAR Global. Orange: NCAR Regional. Green: GOES. (a) March 2006.

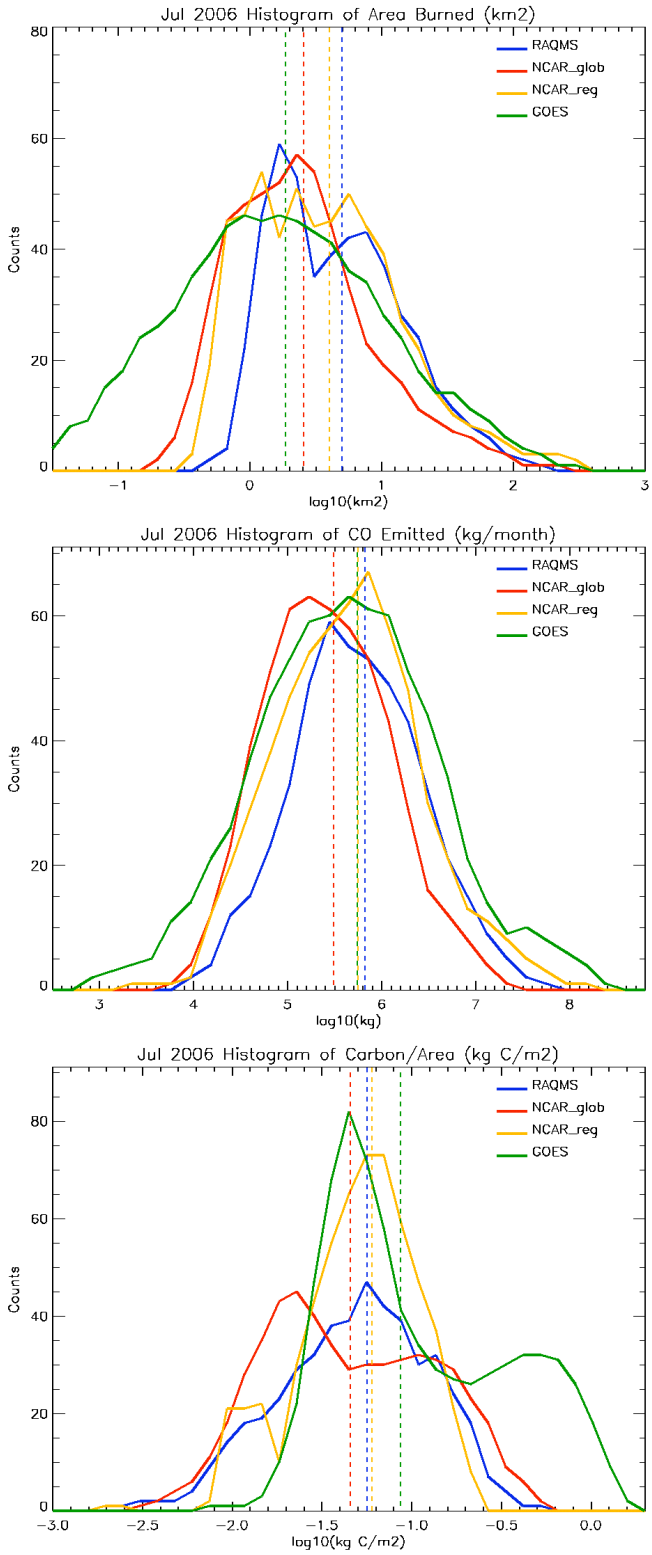

Fig. 5 Concluded. (b) July 2006.

July histograms are shown in Fig. 5(b). The shapes of the area histograms are more similar in July than in March because the peak in the GOES distribution has shifted to larger values and because all methods show a tail of high values associated with the significant wild fire activity in the Pacific Northwest. The CO emission distributions have similar shapes although the GOES distribution is broader and the RAQMS distribution narrower than the others. The NCAR Global distribution is skewed towards lower CO emissions relative to the other distributions. The carbon emissions per unit area in July are quite different from those in March. The GOES distribution is still bimodal but the dominant peak occurs at values similar to NCAR Regional and RAQMS. The NCAR Global distribution is the least changed from

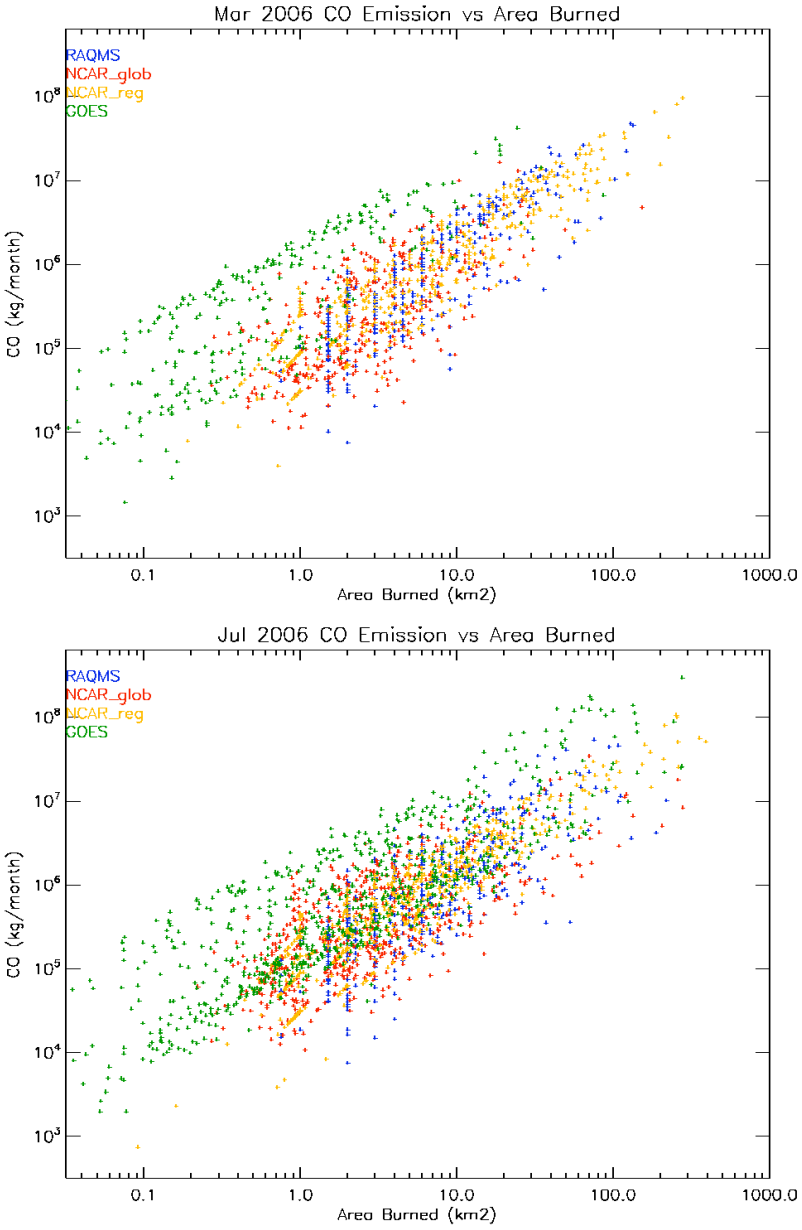

Fig. 6 Scatter plots of CO emitted versus area burned during March and July 2006. Blue: RAQMS. Red: NCAR Global. Orange: NCAR Regional. Green: GOES.

March to July, having a dominant peak at lower values than the other methods during both months.

We further explore the relationships between CO emission and area burned by considering scatter plots for both months in Fig. 6. During March there are two relatively distinct populations apparent in the GOES technique. Within the two populations, CO emissions differ by about an order of magnitude across a wide range of area burned. (This is the cause of the bimodality in the carbon per unit area histograms.) The MODIS-based techniques show a similarly wide range of CO emission values for a given area burned but there are not two distinct populations. Rather, the points are more broadly distributed and shifted toward smaller values of carbon emission and/or larger area burned values, or as noted above, smaller values of carbon emission per unit area. During July these relationships are still evident in the scatter plot, but a larger fraction of the GOES points is in the population having lower emission per unit area.

Several general conclusions can be drawn from these comparisons. The GOES-based technique yields a significant population of fire detections associated with small (less than 1 km^2) area burned estimates. This finding is consistent with the results of Soja et al. [30] who show that the GOES algorithm is capable of detecting a large number of small-scale agricultural fires that are not detected by MODIS (likely due to the continuous observing capability afforded by geostationary orbit, as discussed above). In some regions, apparently associated with forested ecosystems, the GOES technique yields larger values of carbon emission per unit area burned than the other techniques. These differences can not be attributed solely to differences in area burned and so arise at least partially from differences in the carbon emission parameterizations.

This intercomparison shows that a large range of uncertainty exists in the area burned estimates. There is a lack of global ground-based area burned data with which to evaluate these techniques at monthly resolution [21]. Even within the US it is difficult to compile such data because of the different reporting systems in use for different states and ownership categories (e.g., wildland fires versus prescribed and agricultural burns, Federal versus non-Federal land) [26][30]. The National Interagency Fire Center (NIFC) compiles annual totals from all Federal and State agencies reporting within the US [31]. Unofficial totals separated by state are also available and it should be noted that some but not all States include private lands in these totals [32]. Based on these summaries, an estimate of the total area burned over CONUS (i.e., excluding Alaska and Hawaii) for all reported categories of wildland fires during 2006 is 50,465 km^2. For comparison with results shown here, the GFEDv2 results are used to estimate the percentage of 2006 annual area burned that occurred during the 7-month March-September period. The GFEDv2 CONUS estimates for 2006 are 23,147 km^2, 19,327 km^2 or 83.5% of which occurs during March-September. The 7-month totals from all methods are shown along with the scaled NIFC estimate (83.5% of the annual total) in Table 2. These totals vary by a factor of almost 3: estimated NCAR Global and GOES values are about 55%

Table 2. March-September 2006 CONUS total area burned (km^2) estimated from NIFC* and satellite-based methods.

Method	Mar-Sep 2006 Total
NIFC	42,137*
GFEDv2	19,327
RAQMS	38,359
NCAR Global	23,823
NCAR Regional	62,448
GOES	22,480

*see text for details of NIFC estimation

of the NIFC, RAQMS is 90%, and NCAR Regional is 150%. As discussed above, the largest fires dominate monthly (and therefore annual) totals so this evaluation primarily reflects contributions from large fires.

Additional inferences can be made based on previous evaluations. The GOES technique has been evaluated against the 2002 National Wildfire Emission Inventory (NWEI) and 2003-2005 Landsat burn scar data and was found to compare well overall [26]. Largest uncertainty was associated with smallest burn scars. For the largest fires, the GOES estimates were found to be smaller than the NWEI values, consistent with the NIFC comparison shown here. The GFEDv2 estimates have previously been evaluated against annual total values compiled by the NIFC during 2001-2004 [21] and found to have a moderate low bias (17%). The larger low bias shown here for 2006 likely reflects that 2006 was an above-average fire year with a larger burned area than in any of the years 2001-2004 [31]. These evaluations either largely or entirely consider wildland fires. During July, when large wildland fires are known to be major contributors to burning, the estimates shown here vary by a factor of 2 with GFEDv2 on the low side and GOES on the high side of the range. Evaluation during March, when we find differences of about a factor of 10, is even more difficult. The GFEDv2 product is derived using global 500-meter resolution burn scar data from MODIS and would be expected to show some skill at representing small fires, yet no validation is yet available. The GFEDv2 and closely related NCAR Global estimates lie in the lowest third of our reported range in March. The largest uncertainty in the GOES area estimates is associated with the smallest fires, as noted above, and GOES values are the lowest of our range in March. The nominal 1 km^2 burn area per pixel assumed in RAQMS and NCAR global result in the highest March values.

Given the lack of monthly validation data, our overall inference from these comparisons is that the 4 near-real-time methods result in area burned estimates for large fires that are within a spread of plus or minus 50% relative to ground-based observations (which are themselves subject to substantial uncertainty [30]). Regarding small fires, the GOES technique may have a low bias while the assumption of 1 km^2 area burned per MODIS detection may result in a high bias. Area burned estimates in months dominated by small fires have much larger uncertainties (approximately a factor of 10) but contribute relatively little to annual totals.

3.2 Global comparison of CO emissions

Here we briefly compare global emissions from the two global techniques during months where some of the largest burning is occurring. Fig. 7(a) shows CO emissions from RAQMS and NCAR Global during March 2006. This month was the time of largest burning in Southeast Asia. Significant burning was also occurring in the tropics of Africa, Central America, and northern South America. While spatial distributions are quite consistent, emission amounts are clearly much larger in RAQMS over Southeast Asia and Africa. Fig. 7(b) shows emissions for August, the month of peak burning in southern subtropical Africa and second largest month for burning in South America. In regions of largest emissions RAQMS is again higher than NCAR Global. These relative characteristics are similar to those found over CONUS, where the RAQMS emission histogram is shifted toward larger values relative to NCAR Global. Much of the difference in the low-latitude regions of large scale burning is associated with different area burned estimates (not shown). In those regions the current 2-day RAQMS technique yields a larger number of detections than the 8-day CMG product. Also, regions evaluated as having high fire weather severity will likely be assigned larger emissions in the RAQMS technique than would result from the climatology-based approach of NCAR Global.

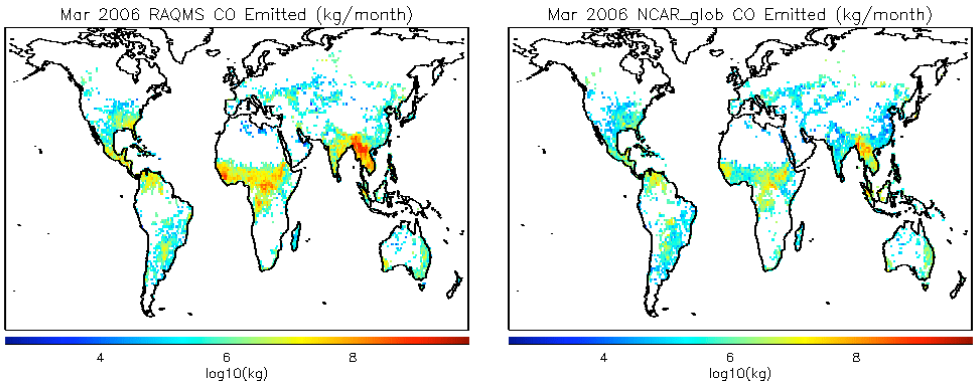

Fig. 7 Global biomass burning CO emissions from RAQMS and NCAR Global techniques. (a) March 2006.

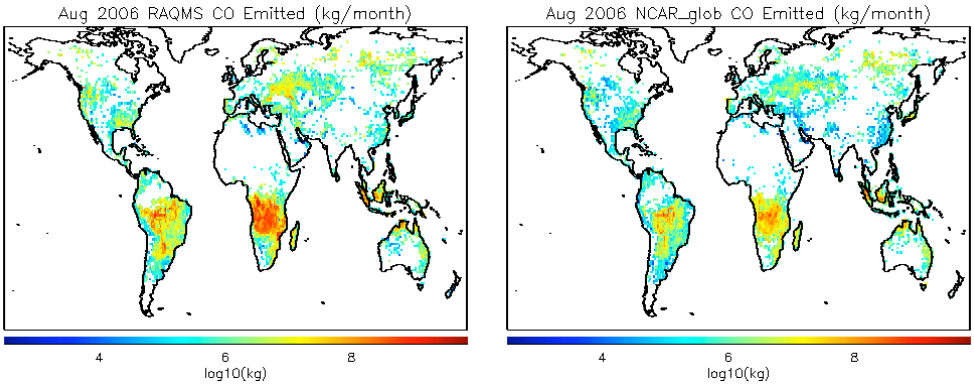

Fig. 7 Concluded. (b) August 2006.

3.3 Evaluation of RAQMS CO emissions

In this section biomass burning CO emissions are evaluated by comparing model CO predictions with satellite CO measurements in regions where CO variability is dominated by biomass burning. We use results from a global 2006 reanalysis conducted with the RAQMS model at a horizontal resolution of 2x2 degrees and using the RAQMS biomass burning emissions presented here. CO profile observations from the Tropospheric Emission Spectrometer (TES) instrument [33] on the Aura satellite have been assimilated in this reanalysis. The TES observation operator is used in the assimilation process to ensure consistency between the vertical resolution of RAQMS and the observations [34][35]. In regions experiencing active burning and where biomass burning is the primary source of CO, the assimilation increment (analysis result after assimilation minus the model first guess) provides a measure of the accuracy of the daily RAQMS biomass burning CO emissions used within the assimilation system.

Fig. 8 shows mean TES-RAQMS CO assimilation increments during March and July. The increments are expressed as percentages of the tropospheric column amounts and positive values indicate that TES observations have larger CO values than the model first guess, suggesting that the emissions have a low bias. In March the burning emissions are largest in the southeast and Fig. 8 shows that first guess CO compares well with TES through much of this region, suggesting that the daily variation and magnitude of the RAQMS burning emissions are realistic. Over Florida and the Gulf Coast the analysis increment is small but

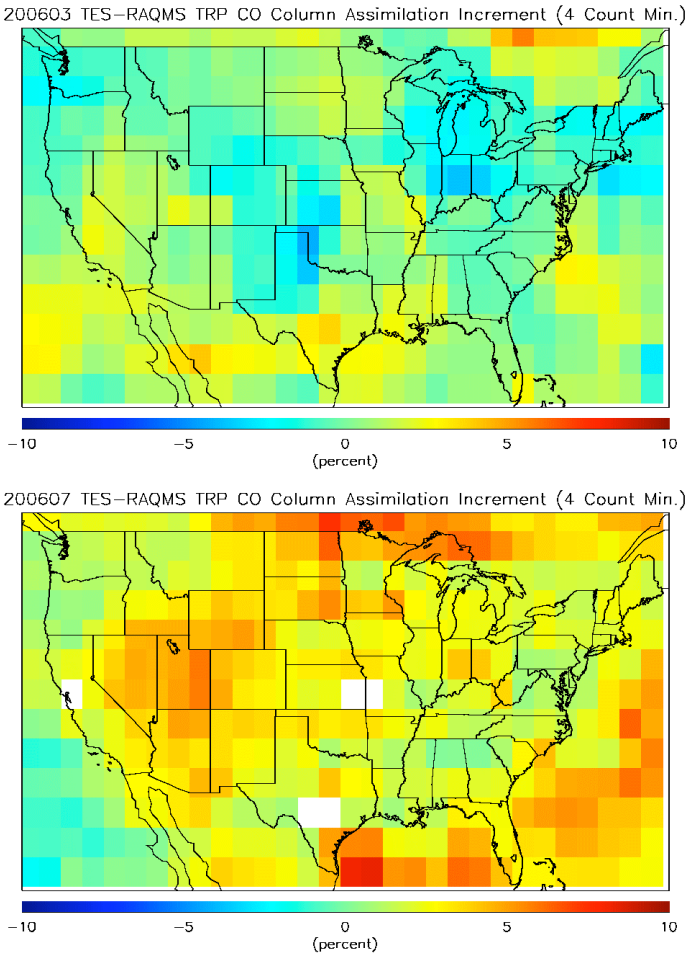

Fig. 8 Monthly mean TES-RAQMS carbon monoxide assimilation increments, expressed as percentages of the tropospheric column amounts, during March (top) and July (bottom) 2006. Positive values indicate that TES observations have larger CO values than the model first guess, suggesting that the emissions have a low bias in regions of burning.

positive (first guess is low relative to TES) with magnitudes of up to 3% of the column, indicating that the RAQMS emissions may have a slight low bias in this region. Over north Texas, where all techniques show a local peak in emissions, the analysis increment is negative 3-5% (first guess is larger than TES), suggesting an overestimate in emissions in that region. During July, when the largest burning emissions are in the west, assimilation increments over burning regions range from zero (northern California, central Oregon) to positive values of up to 5% (Wyoming and Idaho) indicating that the RAQMS emissions may have a low bias in the northwest during this time period.

Fig. 9(a) compares CO column amounts from the RAQMS analysis with MOPITT observations during March 2006, taking into account the *a priori* and averaging kernel information of the MOPITT retrievals [36][37]. Scatter plots of RAQMS versus MOPITT columns are shown over global (lower left panel) and CONUS (lower right panel) domains. Dashed lines show 20% deviations from 1-to-1 lines. Over CONUS the RAQMS analysis is well correlated with MOPITT (r=0.91) but is persistently lower by 20% (mean bias –5.1e17

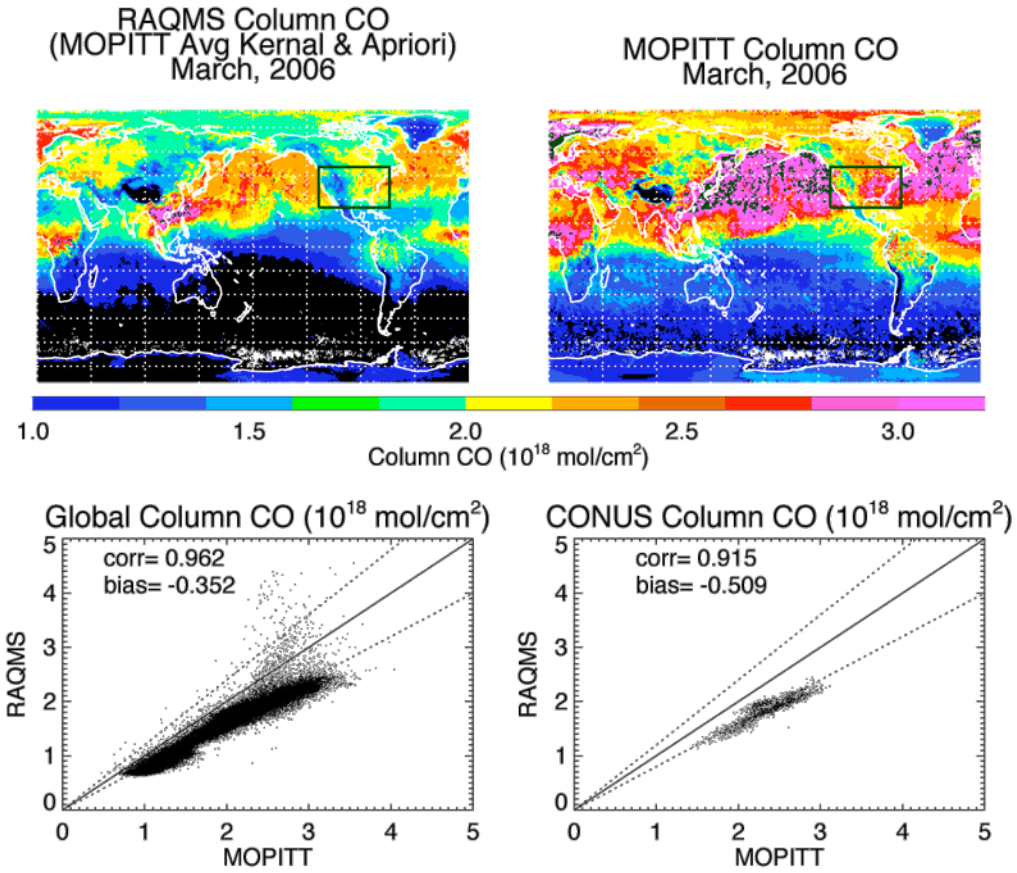

Fig. 9 Comparison of column CO amounts from the RAQMS model and MOPITT observations. Scatter plots show mean statistics over global (bottom left) and CONUS (bottom right) domains. (a) March 2006

molec/cm2). During INTEX-B (March-May 2006) it has been shown that the MOPITT column measurements have a mean high bias of 17.9±12.9% (3.6±2.5 e17 molec/cm2) relative to in-situ measurements over North America and the Pacific [38]. Taken together these evaluations suggest that the RAQMS analysis is consistent with MOPITT observations over CONUS. Globally the mean statistics are also good (r=0.96, mean bias –3.5e17 molec/cm2) but there is a population of points in which the RAQMS CO column is significantly higher than MOPITT. Inspection of the maps (top panels) shows that these points are in the portion of Southeast Asia experiencing large biomass burning (Fig. 7(a)), suggesting that the RAQMS burning emissions are too large there. However there is no indication of an overestimate where large burning is occurring over tropical Africa. Inspection of global TES-RAQMS CO assimilation increments (not shown) supports these findings, with negative assimilation increments as large as 15% of the column over Southeast Asia and smaller increments (between positive and negative 5%) over tropical Africa.

Similar comparisons are presented for August 2006 in Fig. 9(b). Although the overall atmospheric CO column is lower than during March, the correlation and mean bias statistics over CONUS are similar to values in March. Globally there is a much larger population of points in which the RAQMS column is significantly larger than MOPITT. The maps show that these points are in the major burning regions of tropical Africa and South America (evident in Fig. 7(b)). These August MOPITT comparisons are consistent with global TES-

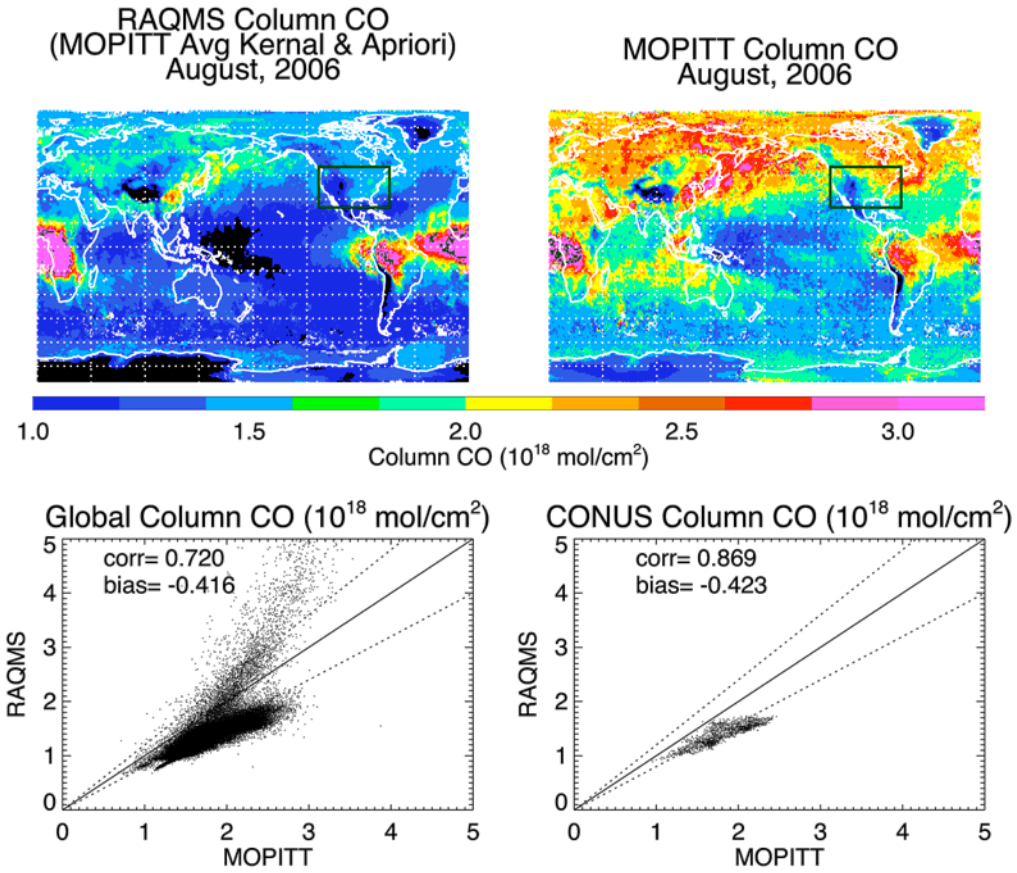

Fig. 9 Concluded. (b) August, 2006.

RAQMS assimilation increments (not shown), which include negative increments in excess of 10% and 15% over tropical South America and Africa, respectively.

Overall these evaluations indicate the current RAQMS emission technique is consistent with satellite CO observations over CONUS but is significantly overestimating emissions in 3 out of 4 major tropical burning events. While this suggests there is either an ecosystem or seasonal dependence to the bias within tropical regions, we have yet to determine whether the tropical biases are associated with overestimates of area burned, emissions per unit area burned, or a combination. Possible causes include smaller area burned per fire detection (associated with short duration fires or slow fire rate of spread), inaccuracies in fuel and/or combustion efficiency parameters in one or more tropical ecosystems, and inaccurate fire severity estimates associated with application of the Haines Index in tropical regions.

4 CONCLUSION

We have analyzed area burned and CO emission estimates resulting from four different techniques that use satellite fire data in near real time to constrain area burned. The analysis is primarily focused on the contiguous US but we also examine global estimates to extend the range of parameters important in characterizing biomass burning emissions. Our primary findings are summarized as follows:

1. Over CONUS there is a wide spread in area burned estimates with a significant fraction of area-burned estimates from GOES smaller than 1 km^2. The GOES technique employs a sub-pixel algorithm to determine instantaneous fire sizes and infer area burned, while the MODIS-based techniques associate a burn area on the order of 1 km^2 with fire detections. Estimates of total area burned are strongly influenced by large fires and the techniques show more consistency during months when large fires occur. Largest uncertainties are associated with small short-duration fires and largest differences are found in months where such fires predominate.
2. CO emissions are more consistent than area estimates over CONUS. This is a result of significant differences among the models in net CO emission rates per unit area within particular ecosystems and vegetation classes. Visual inspection of ecosystem maps suggests largest differences are associated with forested land. The net effect is that differences in CO emission rates are likely compensating for differences in area burned estimates.
3. Based on a 2006 RAQMS model reanalysis, the RAQMS biomass burning CO emissions have a slight low bias over CONUS, resulting in underestimates of tropospheric column CO of up to 5%. Globally, RAQMS has a high bias in CO emissions during 3 of 4 times and locations of large tropical biomass burning, demonstrating an ecosystem or seasonal dependence within tropical regions. At this time we have not determined whether these biases are associated with area burned, the fuel or combustion estimates, or a combination of factors.

Biomass burning emissions have traditionally been represented in large-scale chemical transport models using fire climatologies. This methodology does not take into account the inherent annual variability of fire, particularly in temperate and boreal regions, or future climate-induced change. Within the terrestrial fire community, detailed models incorporating comprehensive ecosystem knowledge have been developed for use in emissions and carbon balance models, but these are often spatially limited. Satellite observations can provide larger scale information on daily to interannual variability of burning, offering a significant improvement on static climatological inventories. In particular the current sensors in polar and geostationary Earth orbits offer complementary observations. The techniques presented in this investigation all represent initial attempts to incorporate information from these communities, and we find that order of magnitude differences can be expected in the resulting estimates of area burned and CO emission. Ultimately, reducing these uncertainties is expected to benefit scientific communities including air quality assessment and forecasting, land cover/land use, carbon cycle and climate change.

Acknowledgements

This work was conducted with support from the NASA Applied Sciences Program. The views, opinions, and findings contained in this article are those of the authors and should not be construed as official National Aeronautics and Space Administration, National Oceanic and Atmospheric Administration, U.S. Environmental Protection Agency, National Center for Atmospheric Research, or U.S. Government position, policy, or decision. The National Center

for Atmospheric Research is operated by the University Corporation for Atmospheric Research under sponsorship of the National Science Foundation.

References

[1] G. R. van der Werf, J. T. Randerson, L. Giglio, G. J. Collatz, P. S. Kasibhatla, and A. F. Arellano, Jr., "Interannual variability in global biomass burning emissions from 1997 to 2004," *Atmos. Chem. Phys.* **6**, 3423–3441 (2006).

[2] G. G. Pfister, L. K. Emmons, P. G. Hess, R. Honrath, J.-F. Lamarque, M. Val Martin, R. C. Owen, M. A. Avery, E. V. Browell, J. S. Holloway, P. Nedelec, R. Purvis, T. B. Ryerson, G. W. Sachse, and H. Schlager, "Ozone production from the 2004 North American boreal fires," *J. Geophys. Res.* **111,** D24S07 (2006) [doi:10.1029/2006JD007695].

[3] P. A. Cook, N. H. Savage, S. Turquety, G. D. Carver, F. M. O'Connor, A. Heckel, D. Stewart, L. K. Whalley, A. E. Parker, H. Schlager, H. B. Singh, M. A. Avery, G. W. Sachse, W. Brune, A. Richter, J. P. Burrows, R. Purvis, A. C. Lewis, C. E. Reeves, P. S. Monks, J. G. Levine, and J. A. Pyle, "Forest fire plumes over the North Atlantic: p-TOMCAT model simulations with aircraft and satellite measurements from the ITOP/ICARTT campaign," *J. Geophys. Res.* **112,** D10S43, (2007) [doi:10.1029/2006JD007563].

[4] J. A. Al-Saadi, J. J. Szykman, R. B. Pierce, C. Kittaka, D. Neil, D. A. Chu, L. Remer, L. Gumley, E. Prins, L. Weinstock, C. MacDonald, R. Wayland, F. Dimmick, and J. Fishman, "Improving National air quality forecasts with satellite aerosol observations," *Bull. Am. Met. Soc.* **86**, 1249-1261 (2005).

[5] G. A. Morris, S. Hersey, A. M. Thompson, S. Pawson, J. E. Nielsen, P. R. Colarco, W. McMillan, A. Stohl, S. Turquety, J. Warner, B. J. Johnson, T. L. Kucsera, D. E. Larko, S. J. Oltmans, and J. C. Witte, "Alaskan and Canadian forest fires exacerbate ozone pollution over Houston, Texas, on 19 and 20 July 2004," *J. Geophys. Res.* **111**, D24S03 (2006) [doi:10.1029/2006JD007090].

[6] R. B. Pierce, J. A. Al-Saadi, T. Schaack, A. Lenzen, T. Zapotocny, D. Johnson, C. Kittaka, M. Buker, M. H. Hitchman, G. Tripoli, T. D. Fairlie, J. R. Olson, M. Natarajan, J. Crawford, J. Fishman, M. Avery, E. V. Browell, J. Creilson, Y. Kondo, and S. T. Sandholm, "Regional Air Quality Modeling System (RAQMS) predictions of the tropospheric ozone budget over east Asia," *J. Geophys. Res.* **108**, 8825 (2003) [doi:10.1029/2002JD003176].

[7] C. Kittaka, R. B. Pierce, J. H. Crawford, M. H. Hitchman, D. R. Johnson, G. J. Tripoli, M. Chin, A. R. Bandy, R. J. Weber, R. W. Talbot, and B. E. Anderson, "A three-dimensional regional modeling study of the impact of clouds on sulfate distributions during TRACE-P," *J. Geophys. Res.* **109**, D15S11 (2004) [doi:10.1029/2003JD004353].

[8] R. B. Pierce, T. Schaack, J. A. Al-Saadi, T. D. Fairlie, C. Kittaka, G. Lingenfelser, M. Natarajan, J. Olson, A. Soja, T. Zapotocny, A. Lenzen, J. Stobie, D. Johnson, M. A. Avery, G. W. Sachse, A. Thompson, R. Cohen, J. E. Dibb, J. Crawford, D. Rault, R. Martin, J. Szykman, and J. Fishman, "Chemical data assimilation estimates of continental U.S. ozone and nitrogen budgets during the Intercontinental Chemical Transport Experiment–North America," *J. Geophys. Res.* **112**, D12S21 (2007) [doi:10.1029/2006JD007722].

[9] Y. Tang, G. R. Carmichael, N. Thongboonchoo, T. Chai, L. W. Horowitz, R. B. Pierce, J. A. Al-Saadi, G. Pfister, J. M. Vukovich, M. A. Avery, G. W. Sachse, T. B. Ryerson, J. S. Holloway, E. L. Atlas, F. M. Flocke, R. J. Weber, L. G. Huey, J. E. Dibb, D. G. Streets, and W. H. Brune, "Influence of lateral and top boundary conditions on regional air quality prediction: A multiscale study coupling regional

and global chemical transport models," *J. Geophys. Res.* **112**, D10S18 (2007) [doi:101029/2006JD007515].

[10] A. J. Soja, R. B. Pierce, J. A. Al-Saadi, E. Alvarado, D. V. Sandberg, R. D. Ottmar, C. Kittaka, W. W. McMillan, G. W. Sachse, J. Warner, and J. J. Szykman, "Description of a ground-based methodology for estimating boreal fire emissions for use in regional- and global-scale transport models," in preparation (2007).

[11] J. S. Olson, "Carbon in live vegetation of major world ecosystems," ORNL-5862, Environmental Sciences Division Publication No. 1997, Oak Ridge National Laboratory, Oak Ridge, Tennessee (1983).

[12] P. J. Zinke, A. G. Strangenberger, W. M. Post, W. R. Emanuel, and J. S. Olson, "Worldwide Organic Soil Carbon and Nitrogen Data," NDP-018, Oak Ridge National Laboratory, Oak Ridge, Tennessee (1986).

[13] A. J. Soja, W. R. Cofer, H. H. Shugart, A. I. Sukhinin, P. W. Stackhouse, Jr., D. McRae, and S. G. Conard, "Estimating fire emissions and disparities in boreal Siberia (1998 through 2002)," *J. Geophys. Res.* **109**, D14S06 (2004) [doi:10.1029/2004JD004570].

[14] D. A. Haines, "A lower atmospheric severity index for wildland fires," *National Weather Digest* **13**, 23-27 (1988).

[15] B. E. Potter, D. Borsum, and D. Haines "Keeping Haines Real–Or Really Changing Haines?," *Fire Management Today* **62**, No. 3, 41-46 (2002).

[16] NASA/University of Maryland, "MODIS Active Fire Detections," Data set, MODIS Rapid Response Project, NASA/GSFC [producer], University of Maryland, Fire Information for Resource Management System [distributors], available on-line <http://maps.geog.umd.edu> (2002).

[17] D. R. Cahoon, Jr., B. J. Stocks, M. E. Alexander, B. A. Baum, and J. G. Goldammer, "Wildland fire detection from space: Theory and application," in *Biomass Burning and its Inter-Relationships with the Climate System*, J. L. Innes, M. M. Verstraete, and M. Beniston (eds.), 151-169, Kluwer Academic, Boston (2000).

[18] L. Giglio, "MODIS Collection 4 Active Fire Product User's Guide Version 2.3," <http://maps.geog.umd.edu/products/MODIS_Fire_Users_Guide_2.3.pdf> (2007).

[19] W. R. Cofer, III, J. S. Levine, E. L. Winstead, and B. J. Stocks, "Trace gas and particulate emissions from biomass burning in temperate ecosystems," in *Global Biomass Burning: Atmospheric, Climatic, and Biospheric Implications*, J. S. Levine (ed.), 203-208, MIT Press, Cambridge, Mass (1991).

[20] M. O. Andreae and P. Merlet, "Emission of trace gases and aerosols from biomass burning," *Global Biogeochemical Cycles* **15** (4), 955–966 (2001).

[21] L. Giglio, G. R. van der Werf, J. T. Randerson, G. J. Collatz, and P. Kasibhatla, "Global estimation of burned area using MODIS active fire observations," *Atmos. Chem. Phys.* **6**, 957–974 (2006).

[22] C. Wiedinmyer, B. Quayle, C. Geron, A. Belote, D. McKenzie, X. Zhang, S. O'Neill, and K. K. Wynne, "Estimating emissions from fires in North America for air quality modeling," *Atmos. Environ.,* **40**, 3419–3432 (2006).

[23] E. M. Prins, C. C. Schmidt, J. M. Feltz, J. S. Reid, D. L. Wesphal, and K. Richardson, "A two-year analysis of fire activity in the Western Hemisphere as observed with the GOES Wildfire Automated Biomass Burning Algorithm," 12th Conf. on Satellite Meteorology and Oceanography, Long Beach, CA, Amer. Meteor. Soc., CD-ROM, P2.28 (2003).

[24] University of Wisconsin, "Biomass burning monitoring page at UW-Madison/ SSEC/ CIMSS," <http://cimss.ssec.wisc.edu/goes/burn/abba.html> (2003).

[25] X. Zhang and S. Kondragunta, "Using GOES Instantaneous Fire Sizes as a Proxy for Burned Areas," GOFC/GOLD 2nd Workshop, Germany, 4-6 December (2006).

[26] X. Zhang and S. Kondragunta, "Temporal and Spatial Variability in Biomass Burned Areas across the USA Derived from the GOES Fire Product," *Remote Sens. Environ.,* Accepted (2008).
[27] X. Zhang and S. Kondragunta, "Estimating forest biomass in the USA using generalized allometric models and MODIS land products," *Geophys. Res. Lett.* **33**, L09402 (2006) [doi:10.1029/2006GL025879].
[28] E. D. Reinhardt, "Using FOFEM 5.0 to estimate tree mortality, fuel consumption, smoke production and soil heating from wildland fire," *Proc. Second International Wildland Fire Ecology and Fire Management Congress and Fifth Symposium on Fire and Forest Meteorology*, Nov. 16-20, 2003, Orlando, FL, Amer. Meteor. Soc. CD-ROM, P5.2 (2003)
[29] S. Korontzi, J. McCarty, T. Loboda, S. Kumar, and C. Justice, "Global distribution of agricultural fires in croplands from 3 years of Moderate Resolution Imaging Spectroradiometer (MODIS) data," *Global Biogeochem. Cycles* **20**, GB2021 (2006) [doi:10.1029/2005GB002529].
[30] A. J. Soja, J. A. Al-Saadi, L. Giglio, D. Randall, G. Pouliot, C. Kittaka, J. Kordzi, S. Raffuse, T. Pace, T. E. Pierce, T. Moore, R. B. Pierce, and J. J. Szykman, "Assessing satellite-based fire data for use in the National Emissions Inventory," this issue.
[31] National Interagency Fire Center, "Fire Information - Wildland Fire Statistics," <http://www.nifc.gov/fire_info/fire_stats.htm> (2007)
[32] National Interagency Coordination Center, "NICC Statistics and Summary: 2006," <http://www.nifc.gov/nicc/predictive/intelligence/intelligence.htm> (2007)
[33] R. Beer, T. Glavich, and D. Rider, "Tropospheric Emission Spectrometer for the Earth Observing System's Aura satellite," *Applied Optics* **40**, 2356–2367 (2001).
[34] D. B. A. Jones, K. W. Bowman, P. I. Palmer, J. R. Worden, D. J. Jacob, R. N. Hoffman, I. Bey, and R. M. Yantosca, "Potential of observations from the Tropospheric Emission Spectrometer to constrain continental sources of carbon monoxide," *J. Geophys. Res.* **108**(D24), 4789 (2003).
[35] K. W. Bowman, C. D. Rodgers, S. S. Kulawik, J. Worden, E. Sarkissian, G. Osterman, T. Steck, M. Lou, A. Eldering, M. Shephard, H. Worden, M. Lampel, S. Clough, P. Brown, C. Rinsland, M. Gunson, and R. Beer, "Tropospheric emission spectrometer: Retrieval method and error analysis," *IEEE Trans. on Geosci. Remote Sensing* **44**(5) (2006).
[36] M. N. Deeter, L. K. Emmons, G. L. Francis, D. P. Edwards, J. C. Gille, J. X. Warner, B. Khattatov, D. Ziskin, J.-F. Lamarque, S.-P. Ho, V. Yudin, J.-L. Attié, D. Packman, J. Chen, D. Mao, and J. R. Drummond, "Operational carbon monoxide retrieval algorithm and selected results for the MOPITT instrument," *J. Geophys. Res*. **108**(D14), 4399 (2003) [doi:10.1029/2002JD003186].
[37] L. K. Emmons, M. N. Deeter, J. C. Gille, D. P. Edwards, J.-L. Attié, J. Warner, D. Ziskin, G. Francis, B. Khattatov, V. Yudin, J.-F. Lamarque, S.-P. Ho, D. Mao, J. S. Chen, J. Drummond, P. Novelli, G. Sachse, M. T. Coffey, J. W. Hannigan, C. Gerbig, S. Kawakami, Y. Kondo, N. Takegawa, H. Schlager, J. Baehr, and H. Ziereis, "Validation of Measurements of Pollution in the Troposphere (MOPITT) CO retrievals with aircraft in situ profiles," *J. Geophys. Res.* **109**, D03309 (2004) [doi:10.1029/2003JD004101].
[38] L. K. Emmons, National Center for Atmospheric Research, Boulder, CO, Private Communication (2007).